

## Chapter 6

# Thermodynamics of Corrosion: Pourbaix Diagrams

### Introduction

Marcel Pourbaix has developed a unique and concise method of summarizing the corrosion thermodynamic information for a given metal in a useful potential–pH diagram. These diagrams indicate certain regions of potential and pH where the metal undergoes corrosion and other regions of potential and pH where the metal is protected from corrosion. Such diagrams are usually called “Pourbaix diagrams” but are sometimes called “equilibrium diagrams” because these diagrams apply to conditions where the metal is in equilibrium with its environment. Pourbaix diagrams are available for over 70 different metals [1].

An example of a Pourbaix diagram is given in Fig. 6.1, which shows the Pourbaix diagram for aluminum. The abscissa in the diagram is the pH of the aqueous solution, which is a measure of the chemical environment. The ordinate is the electrode potential  $E$ , which is a measure of the electrochemical environment. In a Pourbaix diagram, there are three possible types of straight lines:

- (1) Horizontal lines, which are for reactions involving only the electrode potential  $E$  (but not the pH),
- (2) Vertical lines, which are for reactions involving only the pH (but not the electrode potential  $E$ ),
- (3) Slanted lines, which pertain to reactions involving both the electrode potential  $E$  and the pH.

Pourbaix diagrams also contain regions or fields between the various lines where specific chemical compounds or species are thermodynamically stable. The Pourbaix diagram for aluminum in Fig. 6.1 identifies the various regions where the species Al (solid),  $\text{Al}_2\text{O}_3$  (solid),  $\text{Al}^{3+}$  ions, and  $\text{AlO}_2^-$  ions are each stable. When the stable species is a dissolved ion, the region on the Pourbaix diagram is labeled as a region of “corrosion.” When the stable species is either a solid oxide or a solid hydroxide, the region on the Pourbaix diagram is labeled as a region of “passivity,” in which the metal is protected by a surface film of an oxide or a hydroxide. When the stable species is the unreacted metal species itself, the region is labeled as a region of “immunity”. Kruger has described the Pourbaix diagram as being a “map of the possible” [2].

---

*Example 6.1:* After immersion in natural seawater (pH 7.6) for 70 days, the electrode potential of pure aluminum was observed to be  $-1.47$  V vs. SCE [3]. What behavior is expected in terms of corrosion, passivity, or immunity?

*Solution:* First convert the electrode potential to the standard hydrogen scale. From Table 3.2

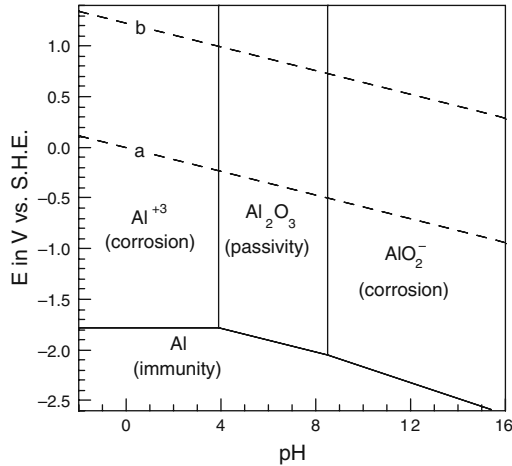


**Fig. 6.1** Pourbaix diagram for aluminum at 25°C. Drawn from data in [1]

$$\begin{aligned}
 E \text{ vs. SCE} &= E \text{ vs. SHE} - 0.242 \\
 -1.47 \text{ V} &= E \text{ vs. SHE} - 0.242 \text{ V} \\
 \therefore E \text{ vs. SHE} &= -1.47 \text{ V} + 0.242 \text{ V} = -1.23 \text{ V}
 \end{aligned}$$

By referring to the Pourbaix diagram for pure aluminum in Fig. 6.1, it is seen that this electrode potential at a pH of 7.6 corresponds to a region of *passivity*.

*Example 6.2:* An Al–1% Mn alloy immersed in 0.1 M sodium citrate solution (pH 3.5) for 24 h displayed an electrode potential of  $-1.25 \text{ V}$  vs. SCE [4]. What behavior is expected in terms of corrosion, passivity, or immunity? What assumptions are you making in your analysis?

*Solution:* First convert the electrode potential to the standard hydrogen scale

$$E \text{ vs. SHE} = -1.25 \text{ V} + 0.242 \text{ V} = -1.01 \text{ V}$$

From the Pourbaix diagram for pure aluminum in Fig. 6.1, it is seen that this electrode potential at a pH of 3.5 corresponds to a region of *corrosion*. The assumptions made are that (1) the Pourbaix diagram for pure aluminum also holds for the dilute Al alloy (1% Mn) and (2) the system is in equilibrium after the relatively short immersion period of 24 h.

## Pourbaix Diagram for Aluminum

### *Construction of the Pourbaix Diagram for Aluminum*

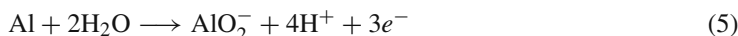
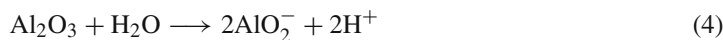
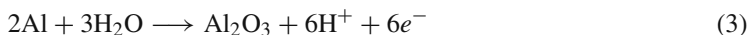
Pourbaix diagrams are constructed from the first principles of thermodynamics. The Pourbaix diagram for aluminum serves as a simple example as to how these diagrams are developed. It is first necessary to assemble the appropriate chemical information about the specific metal being considered. Aluminum undergoes dissolution in acid solutions as  $\text{Al}^{3+}$  ions and in basic solutions as

aluminate ions ( $\text{AlO}_2^-$ ). In neutral or nearly neutral solutions, aluminum is covered with a protective oxide film.

Thus, in the case of the  $\text{Al}/\text{H}_2\text{O}$  system, the various chemical entities and their chemical potentials are as follows [1]:

<i>Dissolved substances</i>	$\mu^\circ(\text{cal/mol})$
$\text{Al}^{3+}$	- 115,000
$\text{AlO}_2^-$	- 200,710
$\text{H}^+$	0
<i>Solid substances</i>	
$\text{Al}$	0
$\text{Al}_2\text{O}_3$	- 384,530
<i>Liquid substances</i>	
$\text{H}_2\text{O}$	- 56,690

The chemical reactions involving these species are [1]



The dissolution of aluminum as  $\text{Al}^{3+}$  ions by Eq. (1) is a reaction involving only the electrode potential  $E$  (but not the pH). We first rewrite Eq. (1) as a reduction reaction. Then, for



the Nernst equation gives

$$E = E^0 - \frac{2.303RT}{nF} \log \frac{1}{[\text{Al}^{3+}]} \quad (7)$$

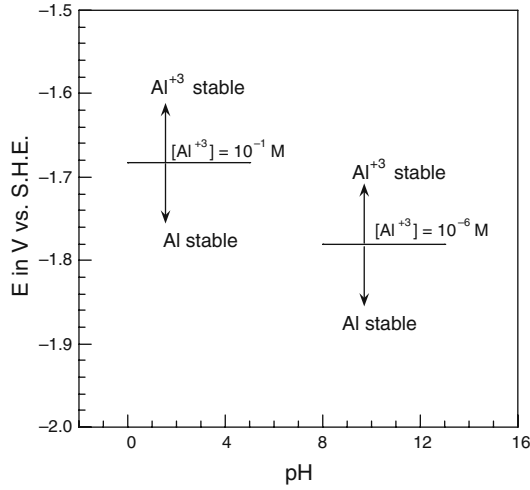
From Table 6.1,  $E^0 = -1.663$  V vs. SHE, and with  $2.303RT/F = 0.0591$  V and  $n = 3$ , Eq. (7) becomes

$$E = -1.663 + 0.0197 \log[\text{Al}^{3+}] \quad (8)$$

The numerical value of the electrode potential  $E$  for the dissolution of Al as  $\text{Al}^{3+}$  ions depends on the concentration of the dissolved ion. Figure 6.2 shows the plot of Eq. (8) for two different values of  $[\text{Al}^{3+}]$ . As seen in Fig. 6.2, the electrode potential for the  $\text{Al}/\text{Al}^{3+}$  reaction becomes more positive with increasing  $[\text{Al}^{3+}]$  concentration. Thus, for a given concentration of  $\text{Al}^{3+}$ , say  $10^{-6}$  M, the oxidized form ( $\text{Al}^{3+}$ ) is stable for potentials above the appropriate straight line at concentrations equal to or greater than  $10^{-6}$  M. Below the given straight line, the oxidized species does not exist at

**Table 6.1** Standard (reduction) potentials for various electrochemical reactions involving aluminum and/or water [1]

Equation number in text	Reaction (oxidation)	$E^0$ (for reduction) (V vs. SHE)
(1)	$\text{Al} \longrightarrow \text{Al}^{3+} + 3e^-$	-1.662
(3)	$2\text{Al} + 3\text{H}_2\text{O} \longrightarrow \text{Al}_2\text{O}_3 + 6\text{H}^+ + 6e^-$	-1.550
(5)	$\text{Al} + 2\text{H}_2\text{O} \longrightarrow \text{AlO}_2^- + 4\text{H}^+ + 3e^-$	-1.262
(22)	$2\text{H}_2\text{O} + 2e^- \longrightarrow \text{H}_2 + 2\text{OH}^-$	-0.828

**Fig. 6.2** Partial Pourbaix diagram for aluminum at 25°C

the concentration being considered. That is, below the straight line, the reduced species (Al atoms) are stable.

A clearer way to see this is to consider an electrode potential which is considerably below the straight line for  $[\text{Al}^{3+}] = 10^{-6}$  M, say  $E = -2.5$  V vs. SHE. Substituting this value of  $E$  into Eq. (8) gives the concentration of  $[\text{Al}^{3+}]$  to be  $2.9 \times 10^{-43}$  M. This is a negligibly small value, so the oxidized species ( $\text{Al}^{3+}$ ) is not stable, and thus the reduced species (solid Al) is stable. In general, for any electrochemical reaction represented on a Pourbaix diagram, the oxidized species of the couple is stable above the straight line of the Nernst equation for the reaction, and the reduced species is stable below the straight line.

By convention, Pourbaix diagrams are usually constructed under the condition that corrosion is considered to have occurred when the minimum concentration of the dissolved ion is  $1.0 \times 10^{-6}$  M. That convention is followed in this text.

Equation (2) is a chemical rather than an electrochemical reaction in that there is no electron transfer involved. The reaction depends on the pH but not on the electrode potential. Thus, from Chapter 4

$$\Delta G^0 = \mu^0(\text{Al}_2\text{O}_3(\text{s})) + 6\mu^0(\text{H}^+(\text{aq})) - [2\mu^0(\text{Al}^3(\text{aq})) + 3\mu^0(\text{H}_2\text{O}(\text{l}))] \quad (9)$$

Using the various values of  $\mu^0$  given earlier gives  $\Delta G^0 = +15,540$  cal/mol  $\text{Al}_2\text{O}_3$  for Eq. (2). Also from Chapter 4

$$\Delta G^0 = -2.303RT \log K \tag{10}$$

where the equilibrium constant  $K$  for Eq. (2) is

$$K = \frac{[H^+]^6}{[Al^{3+}]} \tag{11}$$

Equation (10) yields

$$+ 15,540 \frac{\text{cal}}{\text{mol}} = - 2.303 \left( 1.98 \frac{\text{cal}}{\text{mol. K}} \right) (298 \text{ K}) \log K \tag{12}$$

or

$$\log K = -11.436 \tag{13}$$

Combining Eqs. (11) and (13) gives

$$3 \text{ pH} + \log [Al^{3+}] = 5.718 \tag{14}$$

When  $[Al^{3+}] = 1.0 \times 10^{-6} \text{ M}$ , then Eq. (14) gives the result  $\text{pH} = 3.91$ . This is the pH which results when dissolved  $Al^{3+}$  ions of concentration  $1.0 \times 10^{-6} \text{ M}$  react with water according to Eq. (2). See Fig. 6.3, which summarizes the thermodynamic results so far. It can be shown easily that  $Al^{3+}$  ions are stable to the left of the line  $\text{pH} = 3.91$  and  $Al_2O_3(s)$  is stable to the right of this line. For example, when the pH is 7.0, the concentration of  $Al^{3+}$  calculated from Eq. (14) is  $[Al^{3+}] = 5.2 \times 10^{-16} \text{ M}$ . That is, dissolved  $Al^{3+}$  ions are not stable for pH values greater than 3.91, but instead solid  $Al_2O_3$  is stable in that region.

Continuing with the construction of the Pourbaix diagram for aluminum, we next turn to Eq. (3), which is a reaction depending on both the electrode potential and the pH. After Eq. (3) is first recast as a reduction reaction, writing the corresponding Nernst equation gives

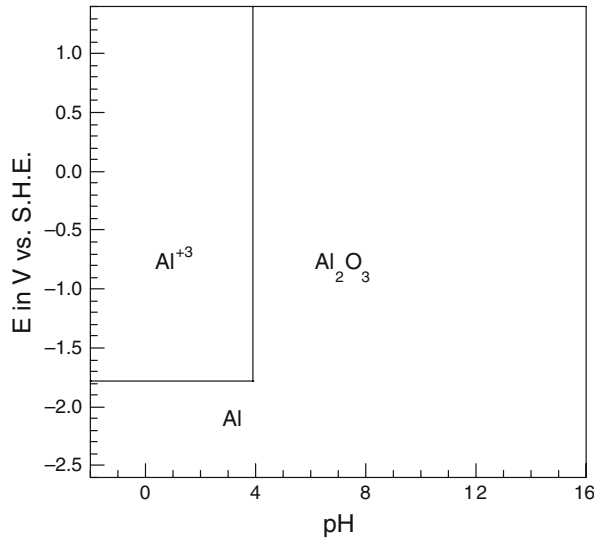


Fig. 6.3 Partial Pourbaix diagram for aluminum at 25°C

$$E = E^{\circ} - \frac{2.303 RT}{nF} \log \frac{1}{[\text{H}^+]^6} \quad (15)$$

The value of  $E^{\circ}$  for Eq. (3) is  $E^{\circ} = -1.550$  V vs. SHE [1]. See Table 6.1. Alternately,  $E^{\circ}$  can be calculated from the free energy change for Eq. (3) using the chemical potentials. This approach is left as an exercise in Problem 6.6. With  $E^{\circ} = -1.550$  V and  $n = 6$ , Eq. (15) gives

$$E = -1.550 - 0.0591\text{pH} \quad (16)$$

See Fig. 6.4, which adds this line to the thermodynamic data accumulated so far and also summarizes the regions of stability for the various species as has been computed so far.

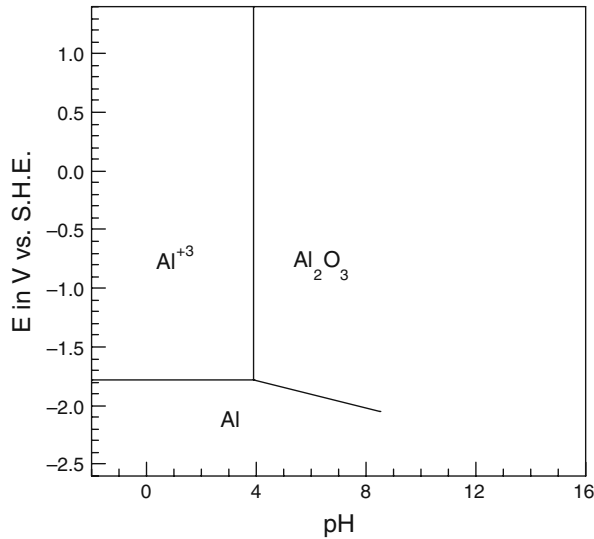


**Fig. 6.4** Partial Pourbaix diagram for aluminum at 25°C

Equation (4) in the set of possible reactions for the Al/H<sub>2</sub>O system can be treated in the same fashion as Eq. (2) because both are chemical (i.e., non-electrochemical reactions). The result for Eq. (4) is

$$-\text{pH} + \log [\text{AlO}_2^-] = -14.644 \quad (17)$$

This result is left as an exercise in Problem 6.7. When the concentration of the dissolved ion, in this case  $\text{AlO}_2^-$ , is  $1.0 \times 10^{-6}$  M, Eq. (17) gives the result

$$\text{pH} = 8.64 \quad (18)$$

The Nernst equation for the electrochemical reaction in Eq. (5) gives the following result

$$E = -1.262 + 0.0197 \log [\text{AlO}_2^-] - 0.0788 \text{pH} \quad (19)$$

See Problem 6.8. When  $[\text{AlO}_2^-] = 1.0 \times 10^{-6}$  M, Eq. (19) gives

$$E = -1.380 - 0.0788\text{pH} \quad (20)$$

Addition of the straight lines for Eqs. (18) and (20) to Fig. 6.4 gives the completed Pourbaix diagram for aluminum shown in Fig. 6.1. The lines labeled “a” and “b” are discussed below.

When the diagram identifies only the regions of corrosion, passivity, and immunity (rather than citing the individual stable species), the diagram is said to be a “simplified Pourbaix diagram.”

### *Comparison of Thermodynamic and Kinetic Data for Aluminum*

According to the Pourbaix diagram in Fig. 6.1, aluminum corrodes only at low pH and at high pH values and does not corrode at pH values between 3.9 and 8.6. This thermodynamic information is in excellent agreement with corrosion rate data for aluminum given earlier in Fig. 2.11 [5]. By referring back to Fig. 2.11, it can be seen that aluminum in aerated 1 M NaCl adjusted to various pH values has its lowest corrosion rates between pH 4 and pH 8.

Figure 6.5 shows additional corrosion data for pure aluminum and an aluminum alloy in aqueous solutions of various pH values [6]. Again, the lowest corrosion rates for aluminum and the aluminum alloy were at intermediate pH values. Thus, while Pourbaix diagrams do not provide actual corrosion rates, the thermodynamic trends given by the Pourbaix diagram are expected to be consistent with the results determined separately for experimental corrosion rates.

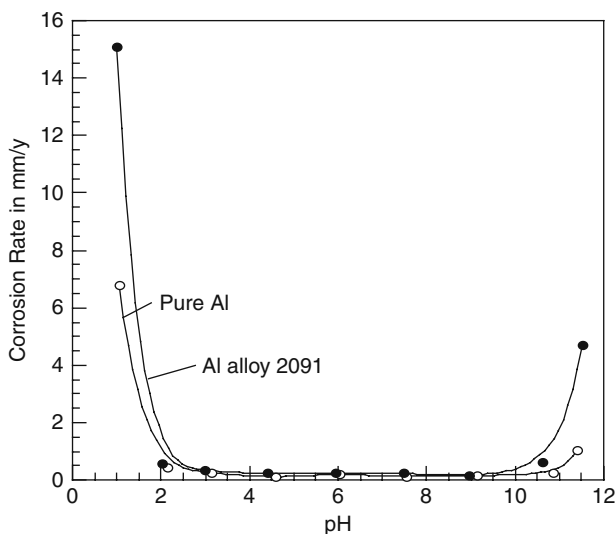


**Fig. 6.5** Corrosion rates of pure aluminum and aluminum alloy 2091 (minor additions of Cu, Li, and Mg and others) in aqueous solutions of various pH values. Redrawn from [6] with the permission of Elsevier, Ltd

### **Pourbaix Diagram for Water**

The line labeled “a” in Fig. 6.1 is for the cathodic evolution of hydrogen. In acid solutions, the cathodic reaction is



and in basic solutions, the cathodic reaction is



For both Eqs. (21) and (22), the Nernst expression at 25°C is

$$E = 0.000 - 0.0591\text{pH} \quad (23)$$

which is plotted as the “a” line in Fig. 6.1. As shown in Fig. 6.6, the reduced species ( $\text{H}_2$ ) in Eqs. (21) or (22) is stable below the “a” line. Above the “a” line, the oxidized species  $\text{H}^+$  is stable in acid solutions, and  $\text{OH}^-$  is stable in basic solutions.

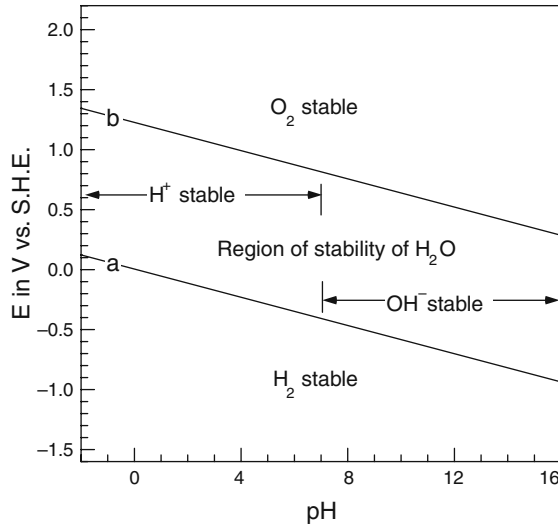


**Fig. 6.6** Pourbaix diagram for water at 25°C [1]

That Eq. (23) also applies to the cathodic reaction in Eq. (22) is posed as Problem 6.9.

The line labeled “b” in Fig. 6.1 is for the anodic evolution of oxygen. At sufficiently high electrode potentials, water molecules dissociate to liberate oxygen by the following anodic reaction:



The Nernst expression for this reaction at 25°C and 1 atm of  $\text{O}_2$  is

$$E = 1.228 - 0.0591\text{pH} \quad (25)$$

Equation (25) is plotted as the “b” line in Figs. 6.1 and 6.6. Below the “b” line the reduced species ( $\text{H}_2\text{O}$ ) is stable, and above the “b” line the oxidized species ( $\text{O}_2$ ) is stable. Between the “a” and “b” lines, water is thermodynamically stable. As stated earlier, below the “a” line,  $\text{H}_2$  evolution is possible; and above the “b” line,  $\text{O}_2$  evolution is possible.

Figure 6.6 is referred to as the Pourbaix diagram for water because this diagram shows region of stability for  $\text{H}_2\text{O}$  (l),  $\text{H}^+$ (aq),  $\text{OH}^-$ (aq),  $\text{H}_2$ (g), and  $\text{O}_2$ (g). The “a” and “b” lines are usually superimposed on the Pourbaix diagrams for metals. The “a” line is of particular interest because it shows conditions where hydrogen evolution is possible. As discussed in Chapter 2, hydrogen atoms are formed by the reduction of  $\text{H}^+$  ions, with two hydrogen atoms combining to form one molecule of



H<sub>2</sub> gas. If, however, some hydrogen atoms migrate into the interior of the metal rather than combining to form H<sub>2</sub>, then the presence of H atoms in stressed regions can promote stress-corrosion cracking by the process of hydrogen embrittlement. Hydrogen embrittlement is a serious form of failure in various metals and alloys, as will be discussed in Chapter 11.

*Example 6.3:* In experiments on the stress-corrosion cracking of 4340 steel (predominately iron with minor amounts of Cr, Mn, and Ni), the local pH of the electrolyte contained within the stress-corrosion crack attained values of 3.0–4.0, even though the pH of the bulk solution was approximately 7. The local electrode potentials corresponding to the pH values of 3.0 and 4.0 were –0.52 V and –0.58 V vs. SCE, respectively [7]. Is hydrogen embrittlement a possible mechanism of stress-corrosion cracking for this alloy?

*Solution:* First convert the electrode potentials to the standard hydrogen scale. For pH 3.0

$$\begin{aligned} E \text{ vs. SCE} &= E \text{ vs. SHE} - 0.242 \\ -0.52 \text{ V} &= E \text{ vs. SHE} - 0.242 \text{ V} \\ E \text{ vs. SHE} &= -0.52 \text{ V} + 0.242 \text{ V} = -0.28 \text{ V} \end{aligned}$$

Similarly, at pH 4.0, the electrode potential is

$$E \text{ vs. SHE} = -0.58 \text{ V} + 0.242 \text{ V} = -0.34 \text{ V}$$

Each of the points (3.0, –0.28) and (4.0, –0.34) when superimposed onto the Pourbaix diagram for water (Fig. 6.6) or for iron (Fig. 6.8) lie below the “a” line for hydrogen evolution. Thus, hydrogen evolution is thermodynamically possible. Accordingly, H atoms can be formed, and hydrogen embrittlement is a possible mechanism of stress-corrosion cracking for this alloy.

## Pourbaix Diagrams for Other Metals

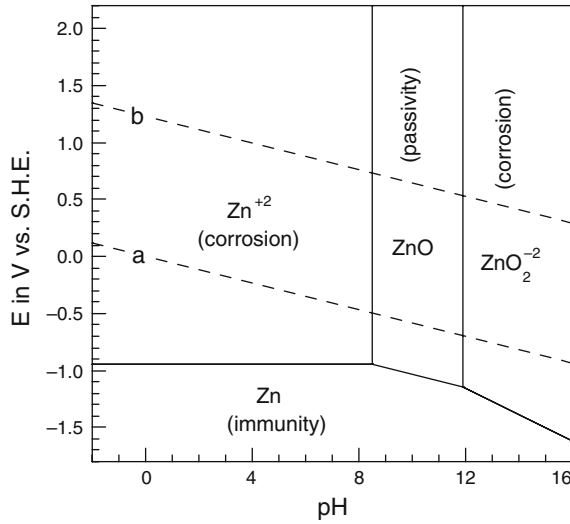
### *Pourbaix Diagram for Zinc*

Figure 6.7 shows the Pourbaix diagram for zinc. (Throughout this chapter, Pourbaix diagrams are calculated using thermodynamic data and electrode potentials given by Pourbaix [1].) The diagram for zinc is similar to that for aluminum because zinc, like aluminum, undergoes dissolution in acid solutions (as Zn<sup>2+</sup> ions) and in basic solutions (as zincate ions, ZnO<sub>2</sub><sup>2-</sup>). This thermodynamic information is in agreement with kinetic data in which zinc has a high corrosion rate at both low and at high pH values, and a lower corrosion rate at intermediate pH values [8].

### *Pourbaix Diagram for Iron*

The Pourbaix diagram for iron is shown in Fig. 6.8. This diagram is of considerable interest because of the widespread use of iron and its alloys as structural materials. Iron can undergo corrosion in acid or neutral solutions in two different oxidation states, i.e., Fe<sup>2+</sup> or Fe<sup>3+</sup>. Passivity is provided by oxide films of Fe<sub>3</sub>O<sub>4</sub> or Fe<sub>2</sub>O<sub>3</sub>. Corrosion in alkaline solutions occurs as the complex anion HFeO<sub>2</sub><sup>-</sup>, which is analogous to the dissolved ions AlO<sub>2</sub><sup>-</sup> and ZnO<sub>2</sub><sup>2-</sup> for aluminum and zinc, respectively, in alkaline solutions.

The Pourbaix diagram for iron shown in Fig. 6.8 is constructed from the set of equilibrium reactions and expressions given in Table 6.2. The simplified Pourbaix diagram for iron shown in Fig. 6.9



**Fig. 6.7** Pourbaix diagram for zinc at 25°C. Drawn from data in [1]

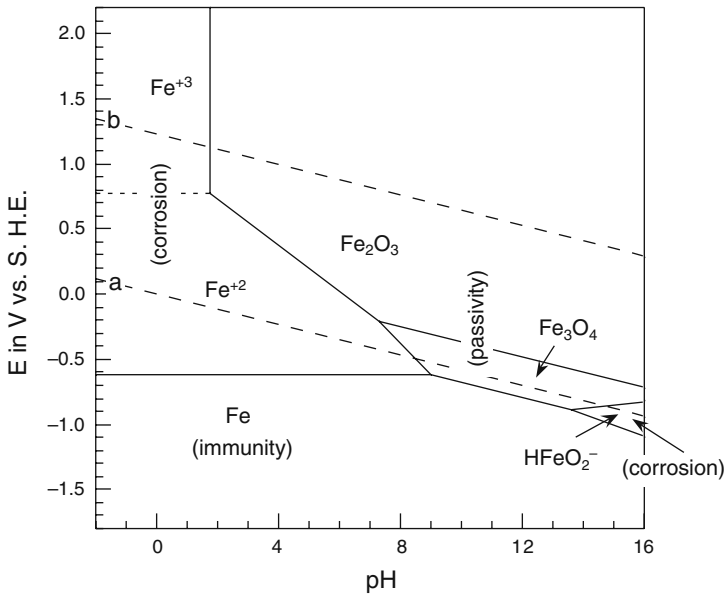


**Fig. 6.8** Pourbaix diagram for iron at 25°C. Drawn from data in [1]

suggests three different means of corrosion protection so as to remove iron from the region of corrosion. For instance, a pH of 6.0 and an electrode potential of  $-0.4$  V vs. SHE corresponds to a region of corrosion as  $Fe^{2+}$  ions. The three corrosion control measures are as follows:

- (1) If the electrode potential is changed in the negative direction to a value below  $-0.7$  V SHE, the iron electrode is forced into a region of immunity. (This process is called *cathodic protection*, which has been discussed earlier in Chapter 5).

**Table 6.2** Equilibrium reactions and thermodynamic expressions for the Fe/H<sub>2</sub>O system [1]

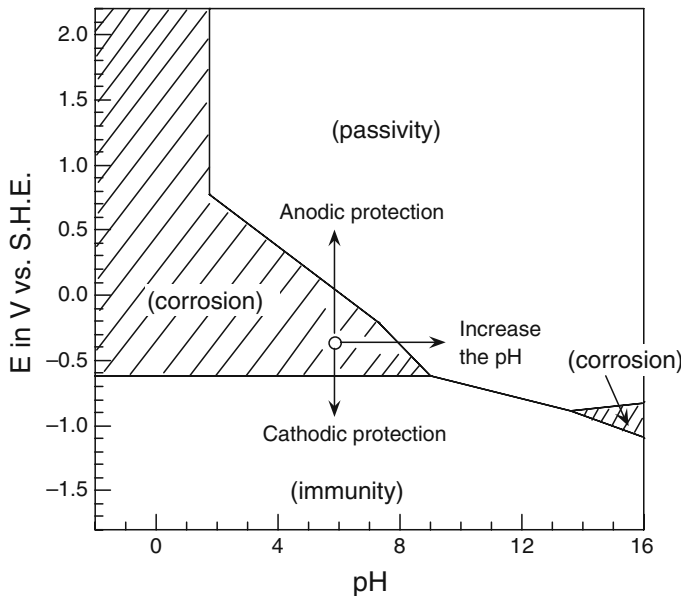
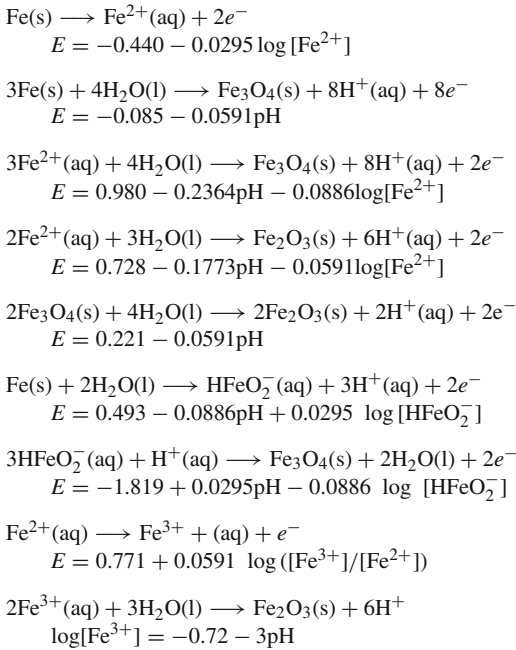


**Fig. 6.9** Simplified Pourbaix diagram for iron at 25°C

- (2) If instead, the electrode potential is changed in the positive direction to values above approximately 0.0 V vs. SHE, the iron electrode is forced into a region of passivity. This process is called *anodic protection* and will be taken up further in Chapter 9.

- (3) The third method of protection is to change the pH of the aqueous solution. If the pH is increased to approximately 8 or higher, the iron electrode will then also reside in a region of passivity.

Figure 6.10 shows a drawing (after Marcel Pourbaix) which illustrates in an amusing but striking manner the differences between immunity, passivity, and corrosion for iron.

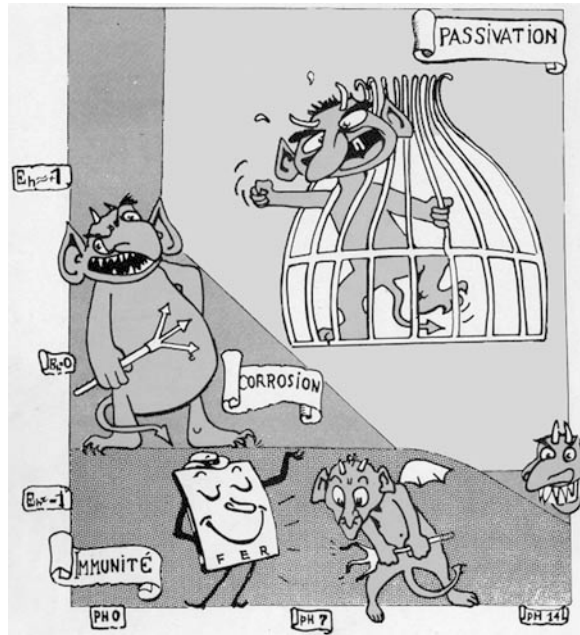


**Fig. 6.10** A humorous look at the Pourbaix diagram for iron (after a colleague of M. Pourbaix). Figure kindly provided by A. Pourbaix of CEBELCOR (Centre Belge d'Etude de la Corrosion)

### *Pourbaix Diagrams for Additional Metals*

The Pourbaix diagram for chromium is shown in Fig. 6.11. A distinguishing feature of this diagram is that the passivity of chromium can be destroyed by increasing the electrode potential (at a given pH). For instance, at pH 7 and an electrode potential of  $-0.4$  vs. SHE, the chromium electrode resides in a region of passivity. But by increasing the electrode potential, the electrode can be shifted into a region of corrosion (as chromate ions). This phenomenon in which corrosion occurs at high electrode potentials (beyond the existence of passivity) is called *transpassive dissolution*.

Figure 6.12 shows the Pourbaix diagram for copper. An interesting feature of the diagram is that the oxidation reactions occur at electrode potentials above the "a" line for hydrogen evolution. Thus, the specific reactions



or



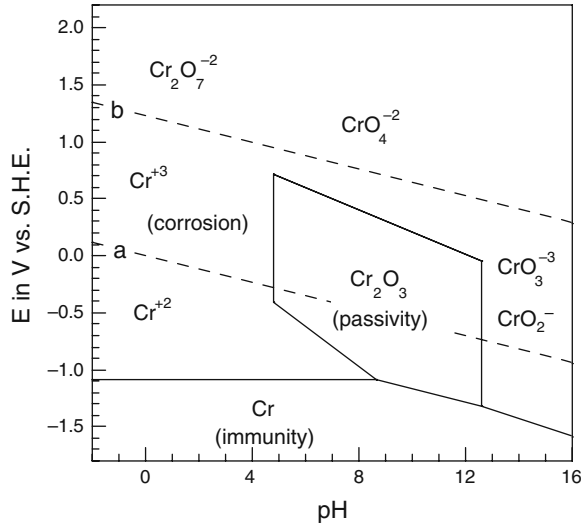
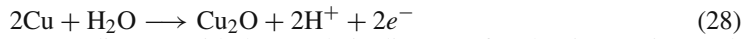


Fig. 6.11 Pourbaix diagram for chromium at 25°C. Drawn from data in [1]

are not thermodynamically favored. That is, copper cannot be oxidized by hydrogen ions or by water molecules to produce H<sub>2</sub> gas (because the product H<sub>2</sub> is not stable in regions where Cu<sup>2+</sup> or Cu<sub>2</sub>O exists). Instead of Eq. (27), the following reaction is favored:



Compare this feature of the copper diagram with the Pourbaix diagrams for aluminum, zinc, and iron, for example.

Figures 6.13 and 6.14 show Pourbaix diagrams for two noble metals silver and palladium, respectively, each of which are used as electronic materials, as dental alloys, and in jewelry. In

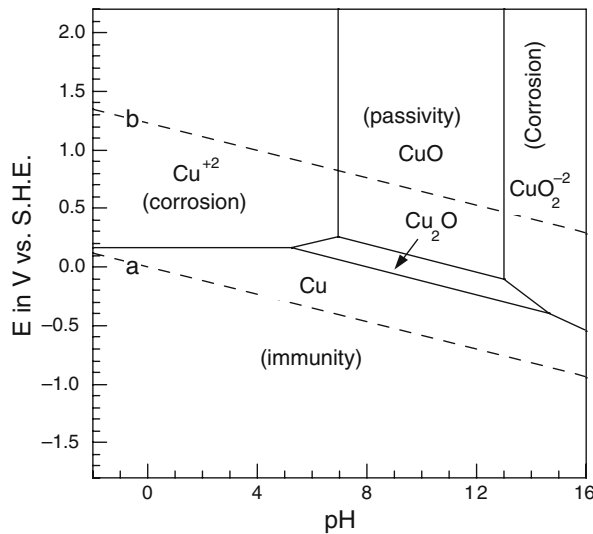
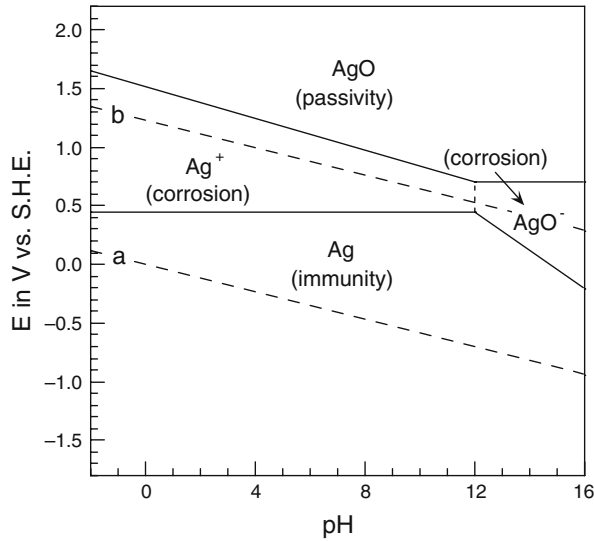


Fig. 6.12 Pourbaix diagram for copper at 25°C. Drawn from data in [1]

addition, palladium finds an important application in catalytic converters used to reduce emissions of hydrocarbons from gasoline-powered vehicles.



**Fig. 6.13** Pourbaix diagram for silver at 25°C (assuming passivity is due to AgO). Drawn from data in [1]

### Applications of Pourbaix Diagrams to Corrosion

Several applications of Pourbaix diagrams to corrosion have already been considered. Various applications can be catalogued as follows [1, 2]:

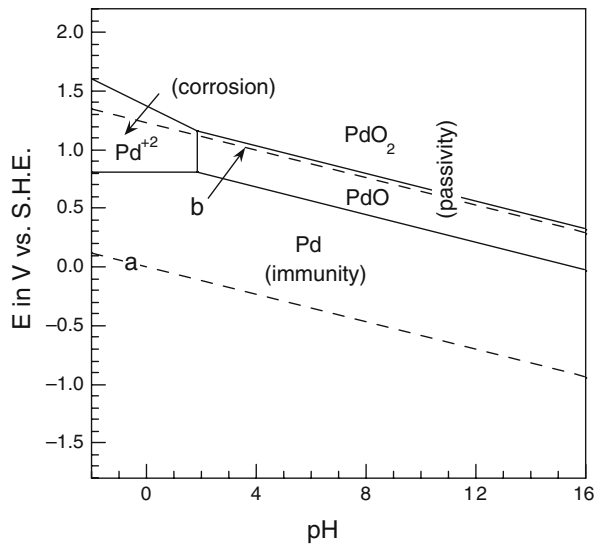


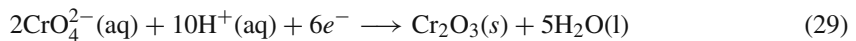
**Fig. 6.14** Pourbaix diagram for palladium at 25°C. Drawn from data in [1]

- (1) The resistance of metals to uniform corrosion in aqueous solutions.
- (2) The basis for establishing which metals can be expected to have passivity over a wide range of conditions of pH and potential.
- (3) Evaluation of the possible use of oxidizing inhibitors.
- (4) Identification of the set of internal conditions within a localized corrosion cell.

The first application listed above, i.e., the corrosion resistance of metals in aqueous solutions has already been treated here in some detail. This method is based on establishing pH–potential domains of corrosion, passivity, and immunity.

The basis for establishing which metals can be passive over a wide range of conditions of pH and potential lies in examining the Pourbaix diagrams for various metals. For instance, the Pourbaix diagram for titanium, given in Fig. 6.15, shows that titanium exhibits passivity over a wide range of pH values due to its stable oxide film, although titanium is susceptible to corrosion in acid solutions. The Pourbaix diagram for tantalum, shown in Fig. 6.16, is even more appealing. As seen in Fig. 6.16, tantalum is either immune to corrosion or forms a passive oxide over the entire potential–pH range. Tantalum is known to be one of the most corrosion-resistant metals available and is used in a variety of applications. However, as pointed out by Macdonald et al. [9], tantalum is subject to corrosion in solutions where the complex ion tantalate ( $\text{TaO}_3^-$ ) can be formed.

An example involving Pourbaix diagrams and corrosion inhibitors is provided by the use of chromates to inhibit the corrosion of iron in nearly neutral solutions. The chromate ion containing  $\text{Cr}^{6+}$  is reduced to  $\text{Cr}^{3+}$  by the following reaction:



(Compare this reaction with the transpassive dissolution of chromium.) By superimposing the region of stability for  $\text{Cr}_2\text{O}_3$  onto the Pourbaix diagram for iron, as in Fig. 6.17, it can be seen that there is a region of overlap where the oxides  $\text{Fe}_2\text{O}_3$  and  $\text{Cr}_2\text{O}_3$  are both stable (the cross-hatched region in Fig. 6.17). In addition, Fig. 6.17 shows that it is possible to prevent the corrosion of Fe

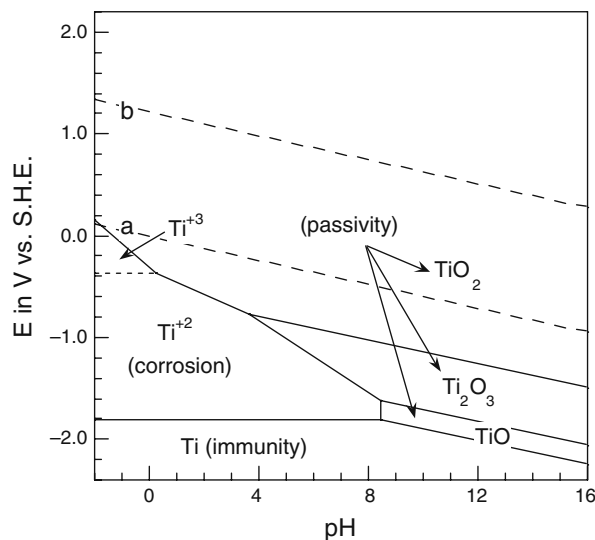


**Fig. 6.15** Pourbaix diagram for titanium at 25°C. Drawn from data in [1]

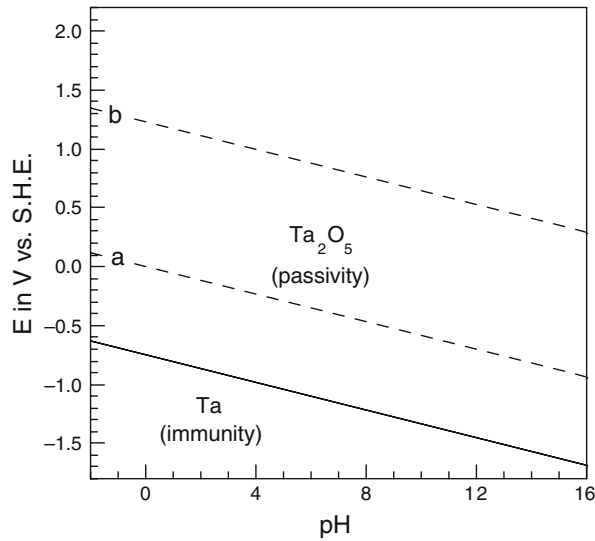


**Fig. 6.16** Pourbaix diagram for tantalum at 25°C. Drawn from data in [1]

as  $\text{Fe}^{2+}$  at approximately neutral pH values through the formation of a  $\text{Cr}_2\text{O}_3$  passive film. The surface analysis of oxide films formed on iron in chromate solutions has shown that the passive film is a bilayer consisting of an outer layer of  $\text{Cr}_2\text{O}_3$  and an inner layer of  $\text{Fe}_2\text{O}_3$  [10]. Thus, films of  $\text{Cr}_2\text{O}_3$  are responsible for corrosion inhibition by chromates, as predicted on the basis of corrosion thermodynamics.

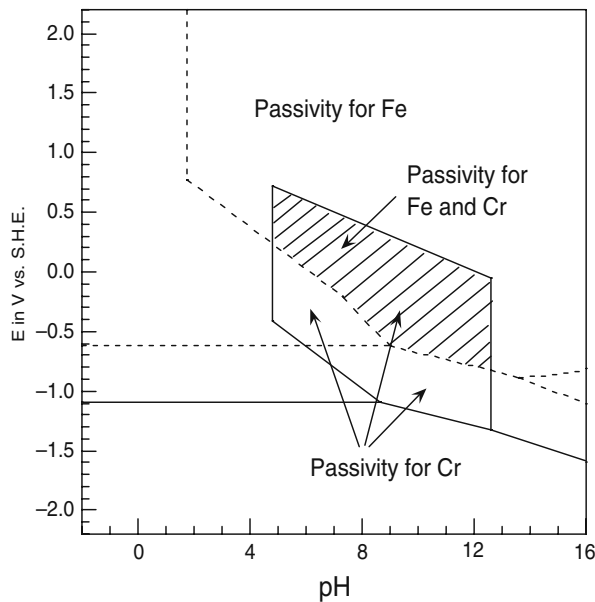


**Fig. 6.17** Superposition of the Pourbaix diagrams for iron (*dotted lines*) and chromium (*solid lines*) at 25°C showing regions of passivity



Pourbaix diagrams can also be applied to localized corrosion processes. Pourbaix diagrams are useful in identifying potential–pH conditions which exist within a localized corrosion cell (crevice, corrosion pit, or stress-corrosion crack), provided that the values of  $E$  and pH pertain to the *local* electrode potential and to the *internal* pH, as in Example 6.3. Further applications to localized corrosion are taken up in Chapter 10 and Chapter 11.

## Limitations of Pourbaix Diagrams

Pourbaix diagrams provide a first guide as to the corrosion behavior of a given metal. Despite their usefulness, as seen above, however, Pourbaix diagrams are subject to several important limitations. These limitations are as follows:

- (1) Equilibrium is assumed. (But in practical cases, the actual conditions may be far from equilibrium.)
- (2) Pourbaix diagrams give no information on actual corrosion *rates*.
- (3) Pourbaix diagrams apply to single elemental metals only and not to alloys. (For a solid solution binary alloy, the Pourbaix diagrams of the two constituents may be superimposed as a first estimate, as will be shown later. For engineering alloys, experimental Pourbaix diagrams may be developed, as will be seen in Chapter 10).
- (4) Passivation is ascribed to all oxides or hydroxides, regardless of their actual protective properties. (Corrosion may sometimes proceed by diffusion of ions through oxide films, a process which is ignored in the construction of the diagrams).
- (5) Pourbaix diagrams do not consider localized corrosion by chloride ions. (Special experimental diagrams must be constructed, as will be seen in Chapter 10.)
- (6) Conventional Pourbaix diagrams apply to a temperature of 25°C. (Pourbaix diagrams exist for elevated temperatures, and examples are given later.)

## *Pourbaix Diagrams for Alloys*

As mentioned above, one of the limitations of Pourbaix diagrams is that the diagrams can be calculated rigorously only for single elemental metals. However, Pourbaix diagrams can be extended to metal alloys by three approaches:

- (1) For binary solid solution alloys, the two individual Pourbaix diagrams may be superimposed onto each other.
- (2) In the case of a mixed binary oxide, the corresponding Pourbaix diagram can be calculated if all appropriate thermodynamic data are available.
- (3) For more complex alloys, including engineering alloys, experimental Pourbaix diagrams can be determined from electrochemical polarization measurements, as will be seen in Chapter 10.

Copper and nickel form solid solution alloys over their entire composition range; so as a first guide as to corrosion trends for Cu-Ni alloys, the Pourbaix diagrams for copper and nickel can be superimposed, as shown in Fig. 6.18. This superposition implies that each of the two metals behaves independently of the other. This assumption is reasonable for solid solution alloys but not for heterogeneous alloys where galvanic effects may arise from the existence of second phases. Figure 6.18 shows that there are regions of potential vs. pH where the preferential dissolution of copper or nickel occurs, as well as regions where both metals undergo dissolution. Films of either

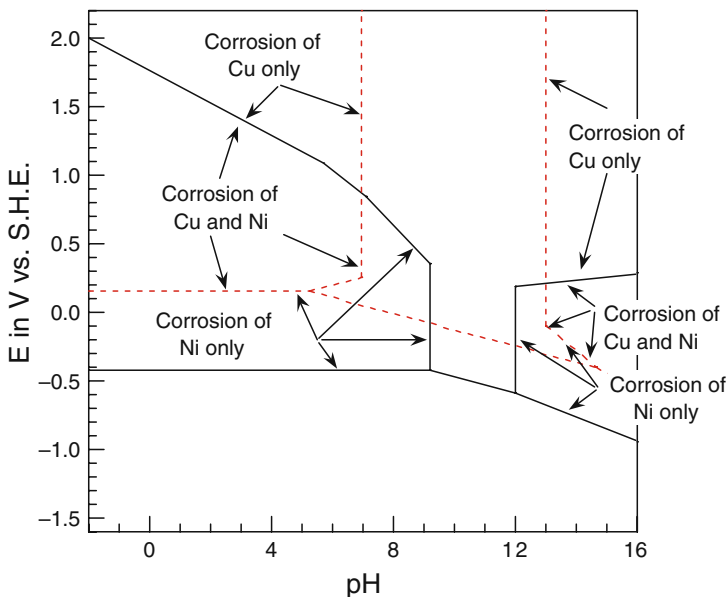


**Fig. 6.18** Superposition of the Pourbaix diagrams for copper (*dotted lines*) and nickel (*solid lines*) at 25°C

$\text{Cu}_2\text{O}$ ,  $\text{CuO}$ , or  $\text{NiO}$  provide passivity at neutral to mildly alkaline pHs. In practice, alloys of Cu–10% Ni and Cu–30% Ni find wide usage in various freshwater and seawater applications.

When thermodynamic information exists for mixed metal oxides, the Pourbaix diagrams can be calculated using such information. Examples include the Fe–Cu– $\text{H}_2\text{O}$  system for the mixed oxide  $\text{FeCuO}_2$  [11] and the Fe–Cr– $\text{H}_2\text{O}$  system for the mixed oxide  $\text{FeCr}_2\text{O}_4$  [12]. Pourbaix diagrams have been computed also for other binary alloys [12] although these diagrams tend to be unduly complex, given their limitations.

## Pourbaix Diagrams at Elevated Temperatures

The construction of Pourbaix diagrams at elevated temperatures is similar to their construction at 25°C, except that it is necessary to add a temperature correction for the free energy change of each individual reaction. The temperature affects:

- (1) the electrode potential  $E$  of electrochemical reactions through the relationship  $\Delta G = -nFE$ , in which the free energy change  $\Delta G$  is a function of temperature,
- (2) the Nernst equation, through the factor  $(2.303RT/F)$ ,
- (3) the equilibrium constant  $K$  in non-electrochemical reactions through the relationship  $\Delta G = -RT \ln K$ , where  $\Delta G$  and (of course)  $T$  are temperature dependent.

Consider the thermodynamic cycle shown in Fig. 6.19, which relates a chemical reaction at 25°C (298 K) to the same reaction at an elevated temperature  $T$ . As shown in Appendix B, the standard free energy change  $\Delta G^\circ_T$  at temperature  $T$  is related to the standard free energy change  $\Delta G^\circ_{298}$  at 25°C by the following expression:

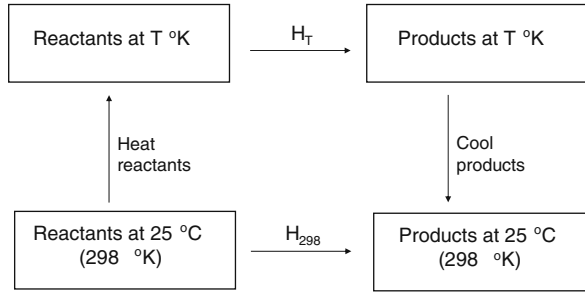


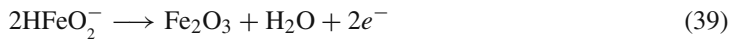
**Fig. 6.19** Thermodynamic cycle for a chemical reaction at two different temperatures

$$\Delta G_T^\circ = \Delta G_{298}^\circ + \int_{298}^T \Delta C_p^\circ dT - T \int_{298}^T \Delta C_p^\circ d \ln T - (\Delta T) \Delta S_{298}^\circ \quad (30)$$

where  $\Delta C_p^\circ$  is a difference in heat capacities given by  $\Delta C_p^\circ = C_p^\circ$  (products) –  $C_p^\circ$  (reactants),  $\Delta T = T - 298$ , and  $\Delta S_{298}^\circ$  is the standard entropy change at 25°C.

The heat capacities required in Eq. (30) are either measured or estimated. Ionic entropies are usually estimated by the empirical correlation method of Criss and Cobble [13, 14] which relates entropies at elevated temperatures to entropies at 298 K.

One of the first Pourbaix diagrams for elevated temperatures was constructed by Townsend [15], who calculated the diagram for iron at temperatures up to 200°C. The 25°C and 200°C diagrams are compared in Fig. 6.20. The two diagrams are similar, with the main difference being that the regime of stability for the complex ion  $\text{HFeO}_2^-$  increases with increasing temperature. In addition, the reaction



was considered to occur at high temperatures but not at 25°C. In the Pourbaix diagram for iron at 200°C, the regions between the complex ion  $\text{HFeO}_2^-$  and the oxides  $\text{Fe}_3\text{O}_4$  and  $\text{Fe}_2\text{O}_3$  are

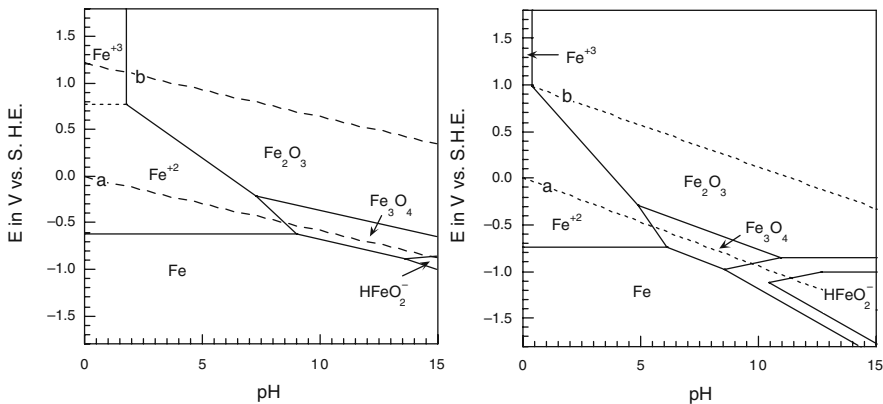


**Fig. 6.20** Pourbaix diagrams for Fe at 25°C (top) and at 200°C (bottom). The bottom figure is redrawn from [15] with the permission of Elsevier, Ltd

shown as bands rather than lines due to uncertainties in the calculation of  $\Delta G^\circ$  as a function of temperature [15].

Pourbaix diagrams have been constructed by Cowan and Staehle [16] for the Ni-H<sub>2</sub>O system in the temperature range of 25–200°C. Analogous to the case for iron, the range of stability of a complex ion  $\text{HNiO}_2^-$  increases with increasing temperature, but for the most part, the Ni-H<sub>2</sub>O diagram at elevated temperatures retains the same general features as the diagram at 25°C.

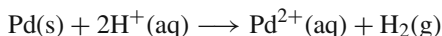
Pourbaix diagrams at elevated temperatures are available for a variety of single metals and alloys [9, 15–19].

## Problems

- The following electrode potentials were observed after a 1-year immersion period in natural seawater of pH 8.0 [20]:

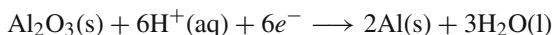
Mild steel	–0.65 V vs. SCE
Zinc	–1.02 V vs. SCE
Mild steel/zinc couple	–0.95 V vs. SCE

- Refer to the appropriate Pourbaix diagrams and indicate what behavior is expected for each of the two uncoupled electrodes. (b) Based on the Pourbaix diagrams, what behavior is expected for the mild steel and zinc components in the short-circuited couple? (c) Is the behavior in part (b) consistent with that predicted based on the galvanic couple approach in Chapter 5?
- Suppose that an acid flux is inadvertently left on the surface of a silver contact and that in the presence of a thin film of condensed moisture, the acid residue has a pH of 5.0. Under what range of electrode potentials could the corrosion of silver occur in the thin-film electrolyte?
  - Palladium (like gold and platinum) is a noble metal. However, the Pourbaix diagram for palladium (Fig. 6.14) contains a region where palladium is subject to corrosion. Can palladium corrode by the following reaction:



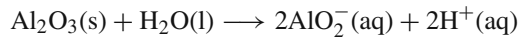
Explain your answer.

- The electrode potential of titanium immersed in a sulfuric acid solution of pH approximately 1 was measured to be –0.70 V vs. SCE [21]. (a) Confirm that titanium undergoes active corrosion under these conditions and (b) consult the Pourbaix diagram to suggest three different means to provide corrosion protection.
- In the interpretation of Pourbaix diagrams, corrosion is considered to occur when the concentration of dissolved metal ions attains a minimum concentration of  $1.0 \times 10^{-6}$  M. Suppose that a 0.50-cm<sup>2</sup> sample of aluminum immersed in 1.0 L of an aqueous solution corrodes at a constant current density of 100  $\mu\text{A}/\text{cm}^2$ . How long will it take to produce a concentration of  $1.0 \times 10^{-6}$  M Al<sup>3+</sup>?
- Calculate the standard reduction potential  $E^\circ$  for the reaction



given the following chemical potentials (in calories per mole):  $\mu^\circ(\text{Al}_2\text{O}_3(\text{s})) = -384,530$ ,  $\mu^\circ(\text{H}_2\text{O}(\text{l})) = -56,690$ .

7. For the chemical reaction



show the result given in Eq. (17), i.e.,

$$-\text{pH} + \log[\text{AlO}_2^-] = -14.644$$

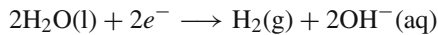
8. For the electrochemical reaction



show the result given in Eq. (19), i.e.,

$$E = -1.262 + 0.0197 \log [\text{AlO}_2^-] - 0.0788 \text{pH}$$

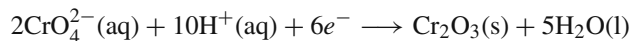
9. For the cathodic evolution of hydrogen from neutral or basic solutions



for which the standard electrode potential is  $E^\circ = -0.828 \text{ V}$  vs. SHE, show that

$$E = 0.000 - 0.0591\text{pH}$$

10. Refer to the Pourbaix diagram for chromium in Fig. 6.11. The equilibrium reaction for the line separating the regions of passivation by  $\text{Cr}_2\text{O}_3$  and transpassive dissolution as chromate ions ( $\text{CrO}_4^{2-}$ ) corresponds to the reaction



Show that the reduction potential for this half-cell reaction depends on both the pH and the concentration of dissolved chromate ions. The standard electrode potential for the reduction reaction is  $E^\circ = 1.311 \text{ V}$  vs. SHE.

11. Refer to Fig. 6.15, which is the Pourbaix diagram for titanium.

(a) Write the electrochemical half-cell reactions for the step-wise oxidation of titanium by the following reactions

Ti (s) to TiO (s)

TiO (s) to  $\text{Ti}_2\text{O}_3$  (s)

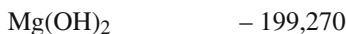
$\text{Ti}_2\text{O}_3$  (s) to  $\text{TiO}_2$  (s)

Note:  $\text{H}_2\text{O}$  is a reactant in each of the above reactions.

(b) What is the slope  $dE/d\text{pH}$  for each of these reactions?

12. The following thermodynamic data are for the Mg/ $\text{H}_2\text{O}$  system [1].

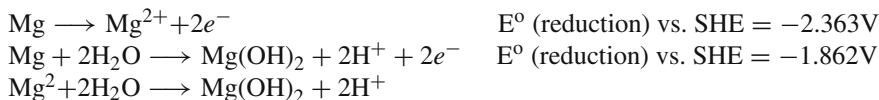
<i>Dissolved substances</i>	$\mu^\circ$ (cal/mol)
$\text{Mg}^{2+}$	- 108,990
$\text{H}^+$	0
<i>Solid substances</i>	
Mg	0



*Liquid substances*



The chemical reactions involving these species are



Calculate and construct the Pourbaix diagram for magnesium, assuming that the passivity of magnesium is provided by a layer of solid  $\text{Mg(OH)}_2$ . Label all regions of corrosion, passivity, and immunity.

13. Construct the Pourbaix diagram for iron from the set of electrochemical and chemical equilibria given in Table 6.2. Label all regions of corrosion, passivity, and immunity.
14. If iron is immersed in a solution of pH 3.0, what electrode potential must be maintained to prevent the evolution of hydrogen gas?
15. In a study on the corrosion of iron in model crevices or pits, Pickering and Frankenthal [22] observed the egress of gas bubbles from the surface of iron contained in the model crevice. For a solution of 0.5 M sodium acetate/0.5 M acetic acid (pH 5.5) contained in the crevice, the electrode potential within the crevice was measured to be  $-0.5$  V vs. SHE [23]. Based on thermodynamic considerations, what gas was evolved?
16. Consult the Pourbaix Atlas [1] or other suitable source for the Pourbaix diagram for niobium. How does this diagram compare with that for tantalum? Based on the location of niobium and tantalum in the periodic table of the elements, would you expect the two Pourbaix diagrams to be similar?

## References

1. M. Pourbaix, "Atlas of Electrochemical Equilibria in Aqueous Solutions", National Association of Corrosion Engineers, Houston, TX (1974).
2. J. Kruger in "Equilibrium Diagrams: Localized Corrosion", R. P. Frankenthal J. Kruger, Eds., p. 45, The Electrochemical Society, Pennington, NJ (1984).
3. R. E. Groover, J. A. Smith, and T. J. Lennox, Jr., *Corrosion*, 28, 101 (1972).
4. E. McCafferty, P. G. Moore, and G. T. Peace, *J. Electrochem. Soc.*, 129, 9 (1982).
5. M. J. Pyror and D. S. Keir, *J. Electrochem. Soc.*, 105, 629 (1958).
6. R. Ambat and E. S. Dwarakadasa, *Corros. Sci.*, 33, 681 (1992).
7. J. A. Smith, M. H. Peterson, and B. F. Brown, *Corrosion*, 26, 539 (1970).
8. T. K. Christman, J. Payer, G. W. Kurr, J. B. Doe, D. S. Carr, and A. L. Ponikvar, "Zinc: Its Corrosion Resistance", pp. 4, 114, International Lead and Zinc Research Institute, New York, NY (1983).
9. H. S. Betrabet, W. B. Johnson, D. D. Macdonald, and W. A. T. Clark in "Equilibrium Diagrams: Localized Corrosion", R. P. Frankenthal and J. Kruger, Eds., p. 83, The Electrochemical Society, Pennington, NJ (1984).
10. E. McCafferty, M. K. Bennett, and J. S. Murday, *Corros. Sci.*, 28, 559 (1988).
11. D. Cubicciotti, *Corrosion*, 44, 875 (1988).
12. D. Cubicciotti, *J. Nucl. Mater.*, 201, 176 (1993).
13. C. M. Criss and J. W. Cobble., *J. Am. Chem. Soc.*, 86, 5385 (1964).
14. J. W. Cobble, *J. Am. Chem. Soc.*, 86, 5394 (1964).
15. H. E. Townsend, Jr., *Corros. Sci.*, 10, 343 (1970).
16. R. L. Cowan and R. W. Staehle, *J. Electrochem. Soc.*, 118, 557 (1971).
17. J. B. Lee, *Corrosion*, 37, 467 (1981).
18. B. Beverskog and I. Puigdomenech, *J. Electrochem. Soc.*, 144, 3476 (1997).
19. R. J. Lemire and G. A. McRae, *J. Nuclear Mater.*, 294, 141 (2001).

20. M. H. Peterson and T. J. Lennox, Jr., *Mater. Perform.*, 23 (3), 15 (1984).
21. M. Stern and H. Wissenberg, *J. Electrochem. Soc.*, 106, 755 (1959).
22. H. W. Pickering and R. P. Frankenthal, *J. Electrochem. Soc.*, 119, 1297 (1972).
23. H. W. Pickering in "Equilibrium Diagrams: Localized Corrosion", R. P. Frankenthal and J. Kruger, Eds., p. 535, The Electrochemical Society, Pennington, NJ (1984).